

OPEN ACCESS

EDITED BY
Osama O. Zaidat,
Northeast Ohio Medical University, United
States

REVIEWED BY Archana Hinduja, The Ohio State University, United States Yuqi Luo, Capital Medical University, China

*CORRESPONDENCE
Bo Xiang

☑ 25286772@qq.com

[†]These authors have contributed equally to this work

RECEIVED 11 April 2025 REVISED 24 October 2025 ACCEPTED 07 November 2025 PUBLISHED 26 November 2025

CITATION

Zhang Z, Yi L, Xiang B and Zhou J (2025) Analysis of 90-day risk factors for poor prognosis in patients with postoperative CT with hyperdense signs after thrombectomy for acute ischemic stroke. *Front. Neurol.* 16:1609722. doi: 10.3389/fneur.2025.1609722

COPYRIGHT

© 2025 Zhang, Yi, Xiang and Zhou. This is an open-access article distributed under the terms of the Creative Commons Attribution License (CC BY). The use, distribution or reproduction in other forums is permitted, provided the original author(s) and the copyright owner(s) are credited and that the original publication in this journal is cited, in accordance with accepted academic practice. No use, distribution or reproduction is permitted which does not comply with these terms.

Analysis of 90-day risk factors for poor prognosis in patients with postoperative CT with hyperdense signs after thrombectomy for acute ischemic stroke

Zhen Zhang[†], Lirong Yi[†], Bo Xiang* and Jie Zhou

Department of Radiology, The Affiliated Yongchuan Hospital of Chongqing Medical University, Chongqing, China

Objective: To investigate the risk factors associated with poor 90-day prognosis in patients exhibiting hyperdense signs on the initial CT scan after mechanical thrombectomy for acute ischemic stroke.

Methods: We conducted a retrospective analysis of 96 patients with acute ischemic stroke who underwent mechanical thrombectomy at The Affiliated Yongchuan Hospital of Chongqing Medical University. The patients were divided into a training set (n = 55, from August 2020 to March 2022) and a validation set (n = 41, from November 2022 to December 2023). Based on the 90d mRS scores, patients were categorized into a good prognosis group (n = 46) and a poor prognosis group (n = 50). Clinical and imaging data were compared between the two groups. A prediction model was constructed using the logistic regression algorithm and validated using the temporal validation method. Receiver operating characteristic (ROC) curves were generated, and the area under the curve (AUC) was calculated to evaluate the discriminative ability of the model. The Hosmer–Lemeshow goodness-of-fit test was used to assess calibration, and decision curve analysis was performed to evaluate the clinical net benefit of each model across various threshold probabilities.

Results: Logistic regression analysis identified the following risk factors for poor 90-day prognosis: D-dimer level, admission diastolic blood pressure, preoperative NIHSS score, vascular occlusion site, as well as the volume of hyperdense areas and the total volume of both hyperdense and hypodense areas on the first postoperative CT scan. Two models were developed: one based solely on an imaging indicator (total volume) and another incorporating combined indicators (total volume, D-dimer, admission diastolic blood pressure, preoperative NIHSS score, and vascular occlusion site). The combined-indicator model demonstrated superior performance. In the training set, it achieved an AUC of 0.886 (95% CI: 0.801–0.971, p < 0.001), accuracy of 0.818, sensitivity of 0.818, and specificity of 0.818. In the test set, the AUC was 0.848 (95% CI: 0.730–0.966, p < 0.001), with an accuracy of 0.707, sensitivity of 0.542, and specificity of 0.941. Decision curve analysis confirmed that two models maintained a positive clinical net benefit within a wide range of threshold probability values (10%–90%).

Conclusion: Patients with hyperdense signs on the first postoperative CT scan exhibit distinct risk factors for poor 90-day prognosis. Combining imaging

features with clinical indicators significantly improves the predictive value for 90-day outcome after mechanical thrombectomy.

KEYWORDS

mechanical thrombectomy, hyperdense signs, postoperative CT, acute ischemic stroke, risk factors, prognosis

1 Introduction

As a pivotal endovascular treatment for revascularizing occluded vessels, mechanical thrombectomy (MT) has become the first-line therapy for acute ischemic stroke (AIS), achieving high rates of successful recanalization and improved clinical outcomes (1-3). However, postoperative cerebral hemorrhage remains a major complication and a leading cause of poor prognosis after MT (4, 5). Non-contrast computed tomography (CT) is routinely used for postoperative assessment, including the detection of hemorrhage and evaluation of treatment efficacy. Postoperative hyperdense signs on CT may arise from contrast staining, hemorrhage, or a combination of both; however, visual interpretation alone often fails to reliably differentiate these entities (6). These hyperdense signs are observed in 31.2%-87.5% of patients, with approximately 46% progressing to hemorrhagic transformation, yet they exhibit low positive predictive value and specificity (7). Currently, short-interval follow-up imaging serves as the primary clinical method to distinguish contrast extravasation from true hemorrhage, relying on the dynamic changes: contrast media typically wash out rapidly, while hemorrhage persists or expands. This approach, however, delays definitive diagnosis and may impede timely clinical decisionmaking. Furthermore, repeated CT scans increase radiation exposure, underscoring the need for more immediate and reliable prognostic tools.

The presence of hyperdensity reflects underlying blood-brain barrier (BBB) disruption and vascular injury, which permit extravasation of contrast or blood into the brain parenchyma (8, 9). Additionally, hypodense regions often correspond to evolving ischemic edema or necrotic tissue, and their volumetric extent may also serve as an important indicator of tissue vulnerability and clinical outcome. The progression of hemorrhagic transformation can significantly worsen prognosis and offset the benefits of thrombectomy, highlighting the importance of early risk stratification. Although previous studies have reported inconsistent associations between hyperdense signs and clinical outcomes (10-12), most rely on qualitative assessment rather than quantitative volumetric analysis. There is a growing recognition that both hyperdense and hypodense volumes on early postoperative CT may offer predictive value, yet the integration of these imaging biomarkers into multivariable prognostic models remains underexplored.

Accordingly, the present study seeks to develop a logistic regression model that integrates quantitative volumetric measurements of both hyperdense and hypodense regions from the first postoperative CT scan with key clinical variables to predict 90-day functional outcomes after thrombectomy. We seek to develop an early predictive tool that facilitates individualized risk assessment and supports clinical decision-making immediately after thrombectomy.

2 Methods

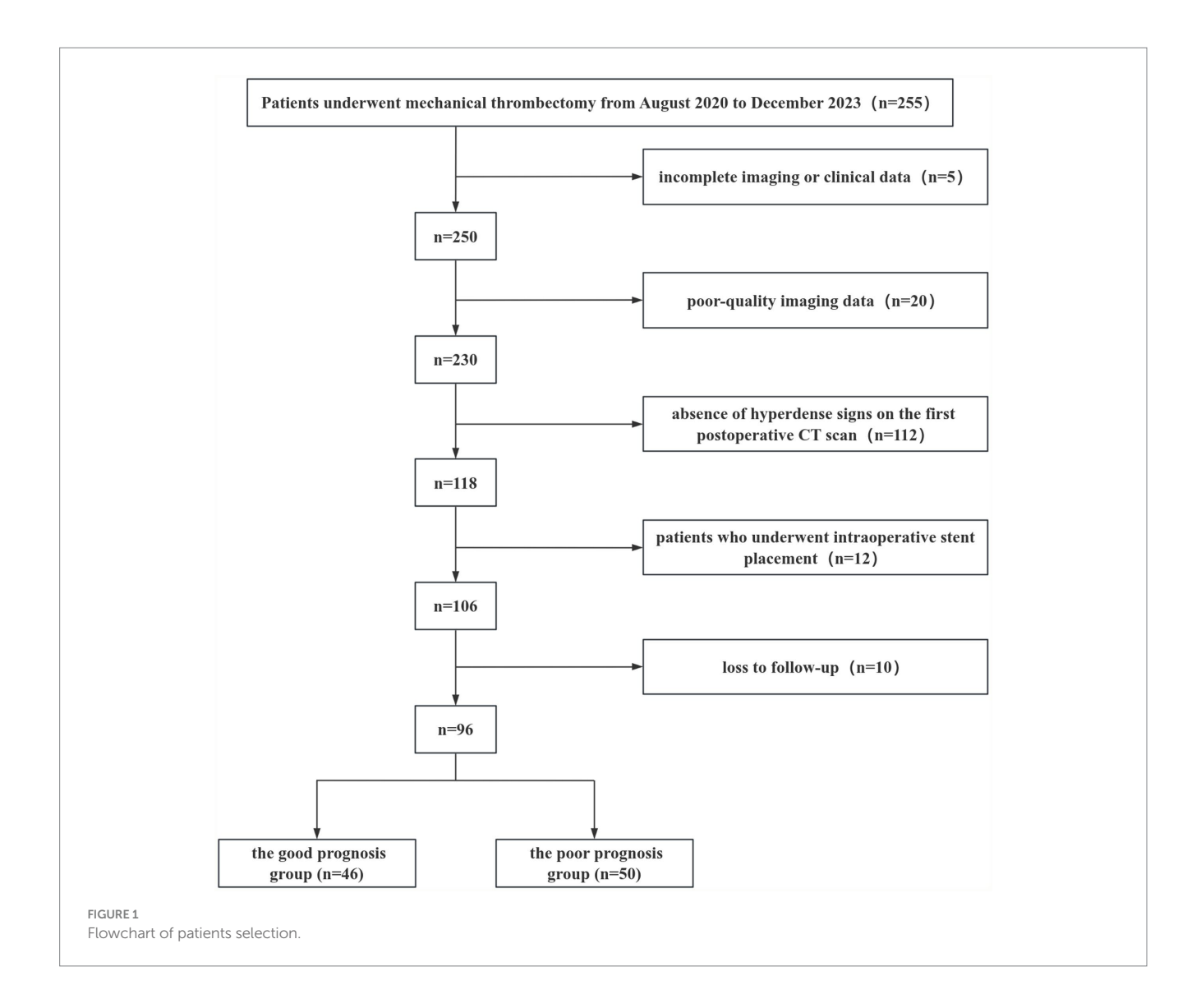
2.1 Patients

A retrospective study was conducted on 96 consecutive patients with acute ischemic stroke who underwent mechanical thrombectomy at The Affiliated Yongchuan Hospital of Chongqing Medical University and presented with hyperdense signs on their first postoperative CT scan. The patients were divided into a training set (n = 55, treated between August 2020 and March 2022) and a validation set (n = 41,treated between November 2022 and December 2023) for temporal validation of the predictive model. Of these, 61 patients (63.54%) were male and 35 (36.46%) were female, with ages ranging from 32 to 101 years (mean age: 66.38 ± 11.58 years). The enrolled patients were followed up and classified into a good prognosis group (mRS 0-2) and a poor prognosis group (mRS 3-6) based on the 90-day postoperative modified Rankin Scale (mRS) score, where a score of 6 indicated death. Inclusion criteria included: (i) Age \geq 18 years; (ii) Confirmed large-artery occlusion based on computed tomography angiography (CTA), magnetic resonance angiography (MRA), or digital subtraction angiography (DSA). Exclusion criteria included: (i) Incomplete imaging or clinical data; (ii) Poor-quality imaging data; (iii) Absence of hyperdense signs on the first postoperative CT scan; (iv) History of intraoperative stent placement; (v) Loss to follow-up (Figure 1). This study was approved by the Ethics Committee of Yongchuan Hospital affiliated with Chongqing Medical University (No. 2024-41).

2.2 Information collection

Clinical and imaging data were collected, including age, gender, medical history, blood pressure, National Institutes of Health Stroke Scale (NIHSS) score, mRS score, volume of high-density areas, volume of low-density areas, and total volume of high-density and low-density areas, among others. Hyperdense signs were defined as hyperattenuating areas present at the thrombectomy site or distributed along the sulci and gyri. Hypodense signs were defined as hypoattenuating areas surrounding the hyperdense areas, with a density lower than that of the contralateral normal brain tissue. This study included patients who underwent mechanical thrombectomy for occlusion of the following major arteries: the middle cerebral artery (MCA), the internal carotid artery (ICA), the intracranial ICA, the intracranial vertebral artery, and the basilar artery.

The region of interest (ROI) was defined on the first postoperative non-contrast CT scan as any area surrounding the surgical cavity exhibiting density alterations relative to normal brain parenchyma. Delineation was performed semi-automatically using uAI-HematomaCare software. The resulting contours were independently reviewed slice by slice by two radiologists, who manually excluded obvious artifacts, pneumatosis within the surgical



tract, and irrelevant calcifications. The following parameters were quantitatively assessed within the finalized ROI: (A) volume of the high-density areas (mL); (B) volume of the low-density areas (mL); (C) total abnormal volume (mL); and (D) mean CT value (HU) of the high-density region.

2.3 Statistical analysis

Statistical analysis was performed using SPSS 26.0 and R version 4.3.0 software. Continuous variables that followed a normal distribution were expressed as mean \pm standard deviation (SD), and comparisons between the two groups were conducted using independent samples t-tests. Continuous variables that did not follow a normal distribution were described as median (interquartile range) [M(P₂₅, P₇₅)], and comparisons were made using the Mann–Whitney U test. Categorical variables were described using frequencies and percentages, and comparisons between groups were performed using the chi-square test. Univariate logistic regression analysis was conducted to identify statistically significant indicators, which were then included in multivariate logistic regression analysis. A *p*-value < 0.05 was considered statistically significant. The diagnostic

performance of the model was evaluated using receiver operating characteristic (ROC) curves and the area under the curve (AUC). Internal validation of the model's differentiation and calibration was performed using Bootstrap method with 500 resamples. The Hosmer–Lemeshow goodness-of-fit test was used to assess calibration, and decision curve analysis (DCA) was employed to evaluate net benefits.

3 Results

3.1 Patients characteristics

Among the 96 patients, 63 (65.6%) had MCA occlusion, 12 (12.5%) had internal carotid artery tandem middle cerebral artery occlusion, 8 (8.3%) had intracranial segment occlusion of the internal carotid artery, 5 (5.2%) had intracranial segment occlusion of the vertebral artery, and 8 (8.3%) had basilar artery occlusion. The good prognosis group comprised 46 patients, including 28 males and 18 females, with a mean age of 63.74 \pm 10.78 years. The poor prognosis group comprised 50 patients, including 33 males and 17 females, with a mean age of 68.8 \pm 11.86 years. Age, history of diabetes, admission diastolic blood pressure, preoperative NIHSS score, preoperative

TABLE 1 Differential analysis of good prognosis group and poor prognosis group.

Parameters	Good prognosis group ($n = 46$)	Poor prognosis group ($n = 50$)	р	
Age (years)*	63.74 ± 10.78	68.80 ± 11.86	0.032	
Sex (male/female)	28/18	33/17	0.602	
Medical history				
Hypertension	26 (56.52)	29 (58.00)	0.884	
Diabetes	5 (10.87)	9 (18.00)	0.035	
Coronary heart disease	4 (8.70)	7 (14.00)	0.183	
Atrial fibrillation	4 (8.70)	7 (14.00)	0.415	
Smoking history	18 (39.13)	26 (52.00)	0.206	
Drinking history	19 (41.30)	25 (50.00)	0.393	
Blood platelet [†]	0.61 (0.30–1.72)	185.50 (149.50-232.75)	0.306	
D-dimer [†]	0.61 (0.30–1.72)	2.05 (0.80-6.78)	< 0.001	
Admission diastolic blood pressure (mmHg)*	140.02 ± 19.17	152.80 ± 25.70	0.007	
Admission systolic blood pressure (mmHg) [†]	82.00 (75.25–89.00)	85.00 (78.00–96.00)	0.226	
Preoperative NIHSS score [†]	14.00 (9.00-17.00)	19.50 (14.00–22.75)	< 0.001	
Preoperative mRS score [†]	4.00 (4.00-4.75)	4.00 (4.00-5.00)	0.026	
Time from onset to femoral artery puncture $(h)^\dagger$	7.00 (4.62–12.75)	7.00 (4.00–10.50)	0.535	
mTICI grade (2b/3)	19/27	20/30	0.760	
Lateral category (unilateral/bilateral)	42/4	41/9	0.183	
Site of vascular occlusion (anterior cerebral circulation/ posterior cerebral circulation)	45/1	38/12	0.002	
First postoperative CT scan				
High density sign CT value (HU) [†]	49.35 (44.55–57.02)	51.95 (48.20–59.77)	0.072	
Volume of high-density areas (mL) [†]	10.05 (3.32-24.60)	33.35 (13.18–63.65)	<0.001	
Volume of low-density areas (ml) [†]	2.75 (0.00-13.60)	4.90 (0.00-34.12)	0.133	
Total volume of high-density and low-density areas (ml) [†]	17.95 (6.22–34.23)	38.75 (16.52–91.78)	< 0.001	

^{*}Data are means \pm SDs, with ranges in parentheses.

mRS score, D-dimer levels, volume of high-density areas, and total volume of high-density and low-density areas were significantly higher in the poor prognosis group compared to the good prognosis group (p < 0.05) (Table 1). Using the time period validation method, the enrolled patients were divided into a training group (n = 55) and a validation group (n = 41) in an approximate 1:1 ratio. No statistically significant differences were observed in clinical data between the two groups (Table 2).

3.2 Risk factor analysis

Statistically significant indicators from the good and poor prognosis groups were included in univariate logistic regression analyses. The results revealed that age, history of diabetes, site of vascular occlusion, D-dimer, admission diastolic blood pressure, preoperative NIHSS score, volume of high-density areas, and total volume of high-density and low-density areas were significant factors associated with poor prognosis in patients with combined hyperdense signs (p < 0.05). Multifactorial logistic regression analysis further demonstrated that site of vascular occlusion, D-dimer, admission diastolic blood pressure, preoperative NIHSS score, volume of

high-density areas, and total volume of high-density and low-density areas were independent risk factors for 90-day poor prognosis in patients with combined hyperdense signs (p < 0.05) (Table 3).

3.3 Model performance

ROC analysis demonstrated that the total volume of hyperdense and hypodense areas exhibited good predictive performance for 90-day poor prognosis in patients presenting with hyperdense signs on the first non-contrast CT scan after mechanical thrombectomy. The AUC was 0.768 (95% CI: 0.641–0.894) in the training set and 0.735 (95% CI: 0.578–0.893) in the validation set. A combined model incorporating vascular occlusion site, D-dimer level, admission diastolic blood pressure, preoperative NIHSS score, hyperdense volume, and total volume of hyperdense and hypodense areas achieved the highest predictive performance, with an AUC of 0.886 (95% CI: 0.801–0.971) in the training set and 0.848 (95% CI: 0.730–0.966) in the validation set (Table 4 and Figure 2).

Internal validation of the model's discrimination and calibration was performed using the bootstrap method with 500 resamples. The model showed strong discriminative ability in

[†]Data are medians, with IORs in parentheses.

TABLE 2 Comparison of clinical data between training and validation groups.

Parameters	Training group ($n = 55$)	Validation group (n = 41)	р
Age (years)*	66.15 ± 12.01	66.68 ± 11.11	0.823
Sex (male/female)	35/20	26/15	0.982
Medical history			
Hypertension	27 (49.09)	28 (68.29)	0.060
Diabetes	11 (20.00)	8 (19.51)	0.953
Coronary heart disease	5 (9.09)	8 (19.51)	0.140
Atrial fibrillation	3 (5.45)	8 (19.51)	0.070
Smoking history	27 (49.09)	17, 41.46	0.458
Drinking history	28 (50.91)	16, 39.02	0.248
Blood platelet [†]	202.00 (161.00-240.00)	172.00 (132.00-211.00)	0.057
D-dimer [†]	1.26 (0.44-4.48)	1.07 (0.40-2.28)	0.493
Admission diastolic blood pressure (mmHg)*	146.36 ± 22.22	147.10 ± 25.56	0.881
Admission systolic blood pressure (mmHg) [†]	84.00 (76.00-93.50)	81.00 (77.00–92.00)	0.447
Preoperative NIHSS score [†]	15.00 (10.00-21.00)	15.00 (11.00–19.00)	0.640
Preoperative mRS score [†]	4.00 (4.00-5.00)	4.00 (4.00-5.00)	0.874
Time from onset to femoral artery puncture $(h)^\dagger$	7.00 (4.00–18.00)	7.00 (4.00–11.00)	0.601
First postoperative CT scan			
High density sign CT value (HU)†	50.90 (46.30-57.05)	50.90 (46.60-59.60)	0.801
Volume of high-density areas (mL) [†]	12.70 (2.85–33.70)	24.30 (5.40–59.10)	0.093
Volume of low-density areas (mL) [†]	3.70 (0.00–19.15)	4.50 (0.00-24.40)	0.912
Total volume of high-density and low-density areas (mL) [†]	19.10 (5.40-43.32)	30.10 (9.70–72.10)	0.203

^{*}Data are means \pm SDs, with ranges in parentheses. † Data are medians, with IORs in parentheses.

TABLE 3 Logistic regression analysis.

Parameters	Single factor			Multifactorial						
	β	SE	Z	р	OR (95%CI)	β	SE	Z	р	OR (95%CI)
Age (years)	0.04	0.02	2.09	0.036	1.04 (1.01-1.08)					
History of diabetes	-1.16	0.57	-2.04	0.041	0.31 (0.10-0.96)					
Site of vascular occlusion	2.65	1.06	2.49	0.013	14.21 (1.77–114.34)	2.59	1.22	2.13	0.033	13.28 (1.23–143.67)
D-dimer	0.26	0.09	2.87	0.004	1.30 (1.09–1.56)	0.26	0.11	2.48	0.013	1.30 (1.06–1.60)
Admission diastolic blood pressure (mmHg)	0.02	0.01	2.58	0.010	1.03 (1.01-1.04)	0.03	0.01	2.43	0.015	1.03 (1.01-1.06)
Preoperative NIHSS score	0.14	0.04	3.63	< 0.001	1.15 (1.07–1.24)	0.12	0.06	2.13	0.033	1.13 (1.01–1.26)
Preoperative mRS score	0.44	0.24	1.80	0.071	1.55 (0.96-2.50)					
Volume of high-density areas (mL)	0.01	0.01	2.08	0.037	1.01 (1.01-1.02)	-0.05	0.03	-2.14	0.033	0.95 (0.90-0.99)
Total volume of high-density and low- density areas	0.02	0.01	2.86	0.004	1.02 (1.01–1.03)	0.06	0.02	3.03	0.002	1.07 (1.02–1.11)

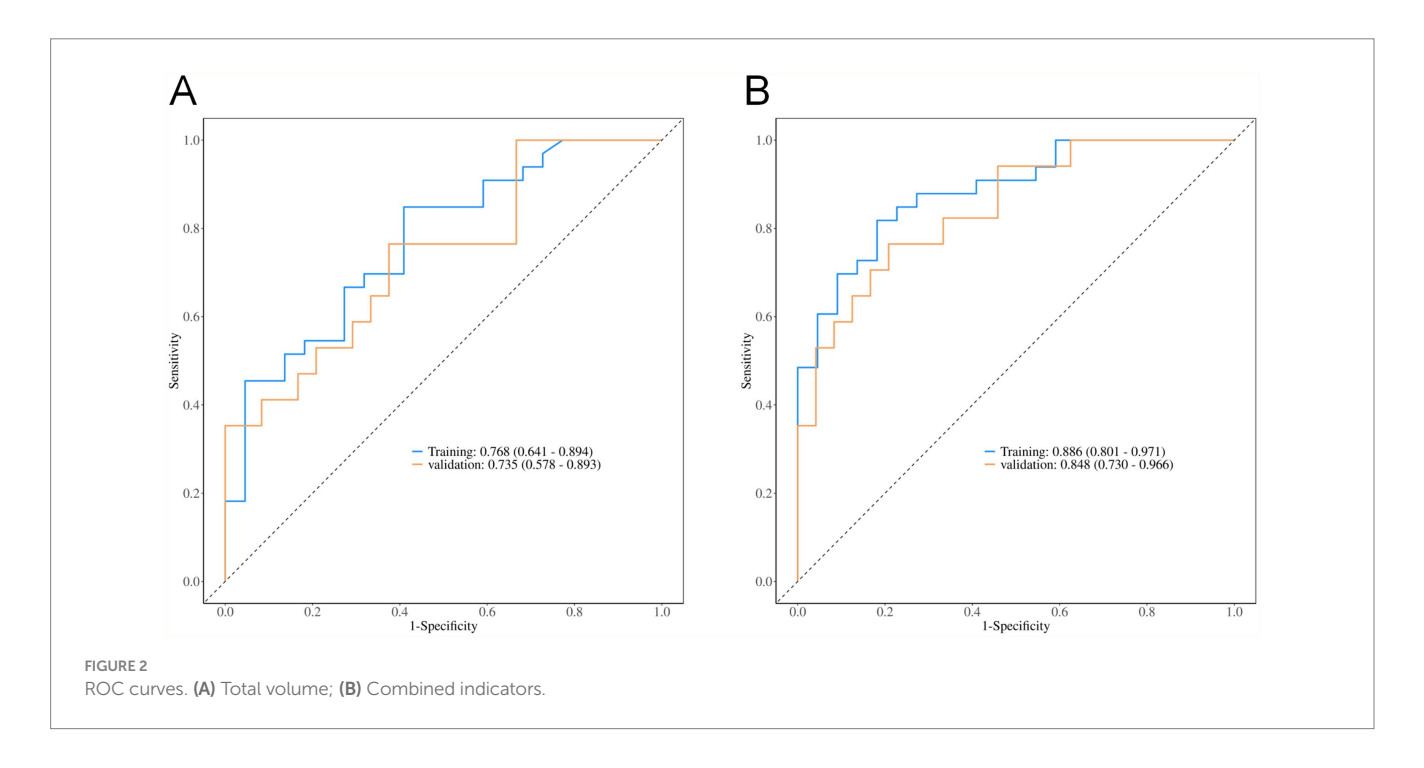
OR, odds ratio; CI, confidence interval.

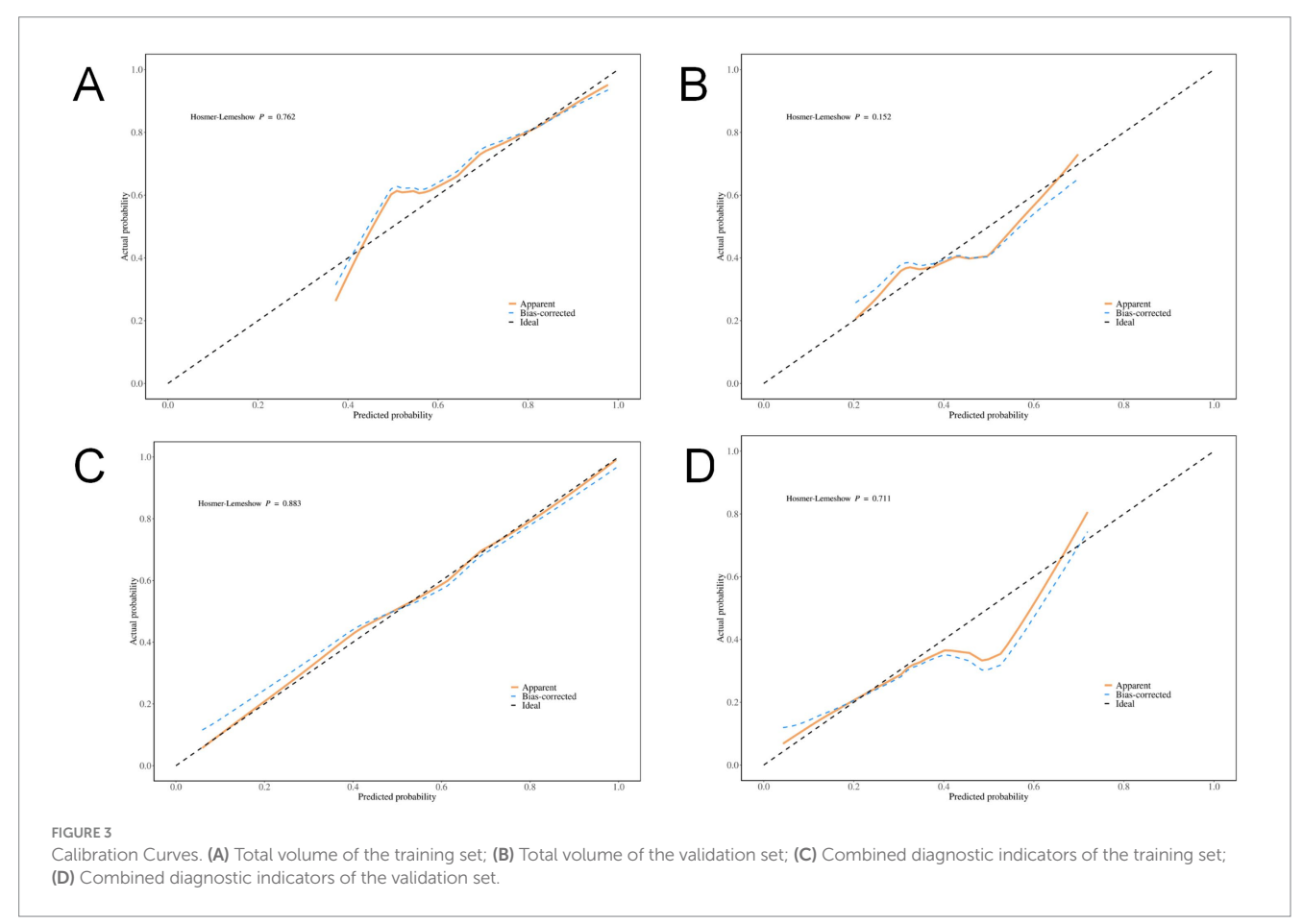
TABLE 4 Predictive efficacy of the model.

Model	Formation	AUC (95% CI)	Accuracy	Sensitivity	Specificity	Cut-off value
Total volume of high-density	Training queue	0.768 (0.641-0.894)	0.745	0.591	0.848	10.9
and low-density zones Validation	Validation queue	0.735 (0.578-0.893)	0.610	0.333	1.000	10.9
Combined indicators	Training queue	0.886 (0.801-0.971)	0.818	0.818	0.818	0.525
	Validation queue	0.848 (0.730-0.966)	0.707	0.542	0.941	0.525

predicting the risk of 90-day poor prognosis among patients with hyperdense signs (p < 0.001, 95% CI: 0.014–0.038). Calibration curve analysis indicated that the predicted probabilities of poor

90-day prognosis from both the combined model and the total volume model were well-aligned with actual outcomes in the training and validation sets (all *p*-values from the





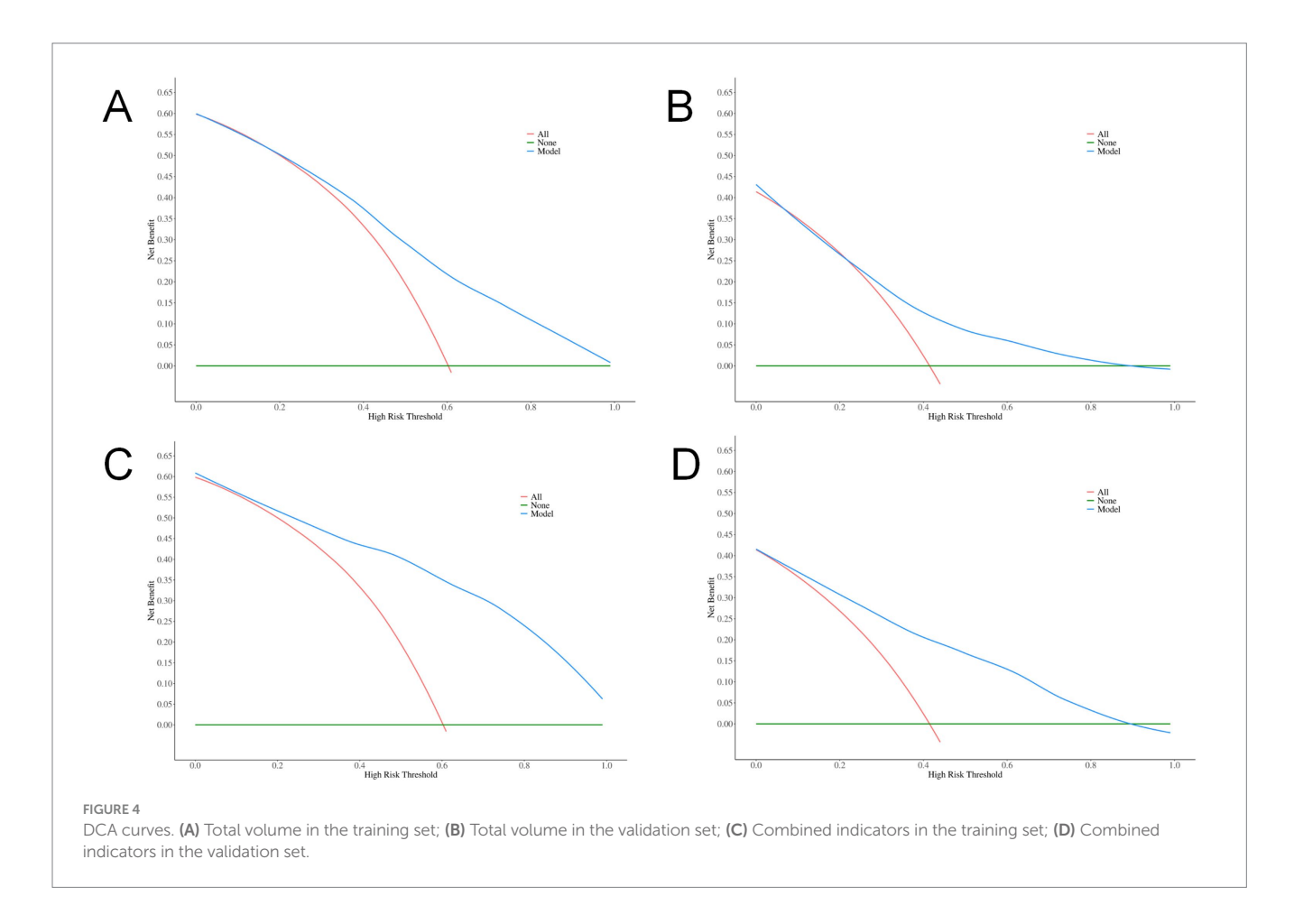
Hosmer-Lemeshow goodness-of-fit test > 0.05, indicating satisfactory calibration performance) (Figure 3).

DCA was conducted to evaluate the clinical utility of the models. The results revealed that both the total volume model (net benefit: 0.135 in the training set, 0.098 in the validation set) and the combined model (net benefit: 0.135 in the training set, 0.086 in the validation set) yielded positive net benefits across a wide range of threshold probabilities (10%–90%), supporting their potential value in clinical decision-making. Notably, the total volume model exhibited a broader range of threshold probabilities with positive net benefit (Figure 4).

4 Discussion

Some researchers have described the high-density areas on CT scan after mechanical thrombectomy as post-intervention cerebral hyperdensities (PCHDs) (13, 14), which may result from contrast staining, hemorrhagic transformation, or a combination of both. PCHDs are primarily associated with BBB disruption. Under normal conditions, the BBB permits the passage of only fat-soluble molecules with a molecular weight < 400 Da, while neither iodine-based contrast agents nor erythrocytes can penetrate it (15, 16). BBB dysfunction can be induced by injury, ischemia, hypoxia, infection, toxins, and other pathological conditions (17, 18). When the damage is confined to vascular endothelial cells, only contrast agents extravasate from the blood vessels. However, when the basement membrane is compromised, both blood components and/or contrast agents may extravasate,

potentially leading to hemorrhagic transformation (19). Previous studies have demonstrated that patients with acute ischemic stroke who undergo mechanical thrombectomy and exhibit high-density CT signs at 24-h follow-up are at increased risk of higher mortality and poorer prognosis (4, 5, 10). Differentiating between postoperative cerebral hemorrhage and contrast extravasation based on conventional CT scans is challenging, as both present as high-density areas. When the CT value exceeds 90 Hounsfield Units (HU), it is often assumed that contrast staining is present, However, the possibility of hemorrhage cannot be entirely excluded. Previous research has predominantly concentrated on the predictive value of hemorrhage and prognosis based on CT scans, emphasizing on the presence of high-density signs and imaging characteristics of hyperdense lesions (including CT values, distribution, shape, and the presence of mass effects). However, few studies have quantitatively assessed changes within and surrounding high-density areas. In this study, volume of high-density areas and total volume of high-density and low-density areas were higher in the poor prognosis group compared to the good prognosis group. The total volume of highdensity and low-density areas demonstrated high specificity (75.8%) in predicting poor prognosis. A higher volume of high-density areas may indicate extensive extravasation of contrast agents and blood components, indirectly reflecting the severity of vascular injury (20). Contrast agents are neurotoxic, and the extravasation of blood components can lead to insufficient reperfusion of surrounding brain tissue and exacerbate inflammatory responses (21). These factors increase the risk of hemorrhage following thrombectomy and worsen cerebral edema. The combined effects of these pathological processes



progressively exacerbate brain tissue damage, which explains why patients with larger total volumes of high-density and low-density areas in this study face a higher risk of poor prognosis. In addition, studies have shown that elevated blood pressure, longer duration from symptom onset, higher preoperative NIHSS scores, and larger cerebral infarct volumes further exacerbate poor outcomes (22-25). In this study, age and preoperative NHISS score were higher in the poor prognosis group compared to the good prognosis group. The American Stroke Association (ASA) notes that elderly patients often exhibit lower vital signs and reduced tolerance to treatment compared to younger patients, leading to a higher likelihood of poor prognosis (26). This observation is largely consistent with the findings of this study. Guidelines indicate that 3-month all-cause mortality is significantly associated with higher or lower baseline blood pressure in patients undergoing endovascular therapy (1). In this study, admission diastolic blood pressure was significantly higher in the poor prognosis group compared to the good prognosis group, a finding consistent with Fu et al's (27) study on risk factors for 90-day mortality after endovascular treatment of ischemic stroke in elderly patients. This may be attributed to the fact that diastolic blood pressure reflects the reserve capacity of the peripheral vasculature, and elevated diastolic blood pressure can impair the reestablishment of blood flow following reperfusion.

This study has several limitations: (i) As a single-center retrospective study with a relatively small sample size, selection bias may be unavoidable. (ii) Due to the limited number of enrolled cases, the analysis did not explore potential differences in influencing factors between patients with anterior and posterior circulation strokes. (iii) Lack of longitudinal follow-up of patients. In conclusion, the total volume of high-density and low-density areas is an independent predictor of poor prognosis. Quantitative assessment of postoperative CT scans provides valuable insights for guiding clinical decision-making and improving patient outcomes.

Data availability statement

The original contributions presented in the study are included in the article/supplementary material, further inquiries can be directed to the corresponding author.

Ethics statement

The studies involving humans were approved by the Medical Ethics Committee of The Affiliated Yongchuan Hospital of Chongqing Medical University. The studies were conducted in accordance with the local legislation and institutional requirements. Written informed consent for participation was not required from the participants or the participants' legal guardians/next of kin in accordance with the national legislation and institutional requirements.

References

1. Chinese Society of Neurology, Chinese Stroke Society, Neurovascular Intervention Group of Chinese Society of Neurology. Chinese guidelines for the endovascular treatment of acute ischemic stroke 2022. *Chin J Neurol.* (2022) 55:565–80. doi: 10.3760/cma.j.cn113694-20220225-00137

Author contributions

ZZ: Conceptualization, Data curation, Formal analysis, Investigation, Methodology, Writing – original draft, Writing – review & editing. LY: Conceptualization, Data curation, Investigation, Methodology, Writing – original draft, Writing – review & editing. BX: Conceptualization, Funding acquisition, Methodology, Project administration, Resources, Supervision, Writing – original draft, Writing – review & editing. JZ: Data curation, Writing – original draft.

Funding

The author(s) declare that financial support was received for the research and/or publication of this article. This research was funded by Chongqing Yongchuan District Natural Science Fund and Chongqing Municipal Science and Health Joint Medical Research Project, grant number 2022yc-jckx20019 and 2025MSXM080.

Acknowledgments

The authors thank all participating patients for their willingness to contribute to medical research.

Conflict of interest

The authors declare that the research was conducted in the absence of any commercial or financial relationships that could be construed as a potential conflict of interest.

Generative AI statement

The authors declare that no Gen AI was used in the creation of this manuscript.

Any alternative text (alt text) provided alongside figures in this article has been generated by Frontiers with the support of artificial intelligence and reasonable efforts have been made to ensure accuracy, including review by the authors wherever possible. If you identify any issues, please contact us.

Publisher's note

All claims expressed in this article are solely those of the authors and do not necessarily represent those of their affiliated organizations, or those of the publisher, the editors and the reviewers. Any product that may be evaluated in this article, or claim that may be made by its manufacturer, is not guaranteed or endorsed by the publisher.

2. Ran, Y, Su, W, Gao, F, Ding, Z, Yang, S, Ye, L, et al. Curcumin ameliorates white matter injury after ischemic stroke by inhibiting microglia/macrophage Pyroptosis through NF-κB suppression and NLRP3 Inflammasome inhibition. *Oxidative Med Cell Longev.* (2021) 2021:1552127. doi: 10.1155/2021/1552127

- 3. Kerleroux, B, Janot, K, Hak, JF, Kaesmacher, J, Hassen, WB, Benzakoun, J, et al. Mechanical Thrombectomy in patients with a large ischemic volume at presentation: systematic review and d-analysis. *J Stroke*. (2021) 23:358–66. doi: 10.5853/jos.2021.00724
- 4. Chen, LL, Yang, WM, Zhang, C, Wang, K, and Wang, JY. Predictive value of non-contrast CT hyperdensity on short-time prognosis after successful recanalization of acute anterior circulation occlusion cerebral infarction. *Chin J Nerv Ment Dis.* (2020) 46:540–5. doi: 10.3969/j.issn.1002-0152.2020.09.007
- 5. He, SW, Wang, CC, Pan, DD, Wang, DW, Zhang, H, Wang, H, et al. Analysis of risk factors for hemorrhage transformation and establishment of risk prediction model after mechanical thrombectomy in acute large vessel occlusion. *Chin J Gen Pract.* (2020) 18:2013–2016,2046. doi: 10.16766/j.cnki.issn.1674-4152.001676
- 6. Cellina, M, Cè, M, Marziali, S, Irmici, G, Gibelli, D, Oliva, G, et al. Computed tomography in traumatic orbital emergencies: a pictorial essay-imaging findings, tips, and report flowchart. *Insights Imaging*. (2022) 13:4. doi: 10.1186/s13244-021-01142-y
- 7. Whitney, E, Khan, YR, Alastra, A, Schiraldi, M, and Siddiqi, J. Contrast extravasation post Thrombectomy in patients with acute cerebral stroke: a review and recommendations for future studies. *Cureus*. (2020) 12:e10616. doi: 10.7759/cureus.10616
- 8. Yedavalli, V, and Sammet, S. Contrast extravasation versus hemorrhage after Thrombectomy in patients with acute stroke. *J Neuroimaging*. (2017) 27:570–6. doi: 10.1111/jon.12446
- Wang, R. Frontal lobe hemorrhage in a patient with lenticulostriate artery territory infarction and middle cerebral artery occlusion after recanalization: a case study and literature analysis. Quant Imaging Med Surg. (2022) 12:2178–83. doi: 10.21037/qims-21-817
- 10. Calloni, SF, Panni, P, Calabrese, F, Del Poggio, A, Roveri, L, Squarza, S, et al. Cerebral hyperdensity on CT imaging (CTHD) post-reperfusion treatment in patients with acute cerebral stroke: understanding its clinical meaning. *Radiol Med.* (2022) 127:973–80. doi: 10.1007/s11547-022-01525-1
- 11. Chen, Z, Zhang, Y, Su, Y, Sun, Y, He, Y, and Chen, H. Contrast extravasation is predictive of poor clinical outcomes in patients undergoing endovascular therapy for acute ischemic stroke in the anterior circulation. *J Stroke Cerebrovasc Dis.* (2020) 29:104494. doi: 10.1016/j.jstrokecerebrovasdis.2019.104494
- 12. Dekeyzer, S, Nikoubashman, O, Lutin, B, De Groote, J, Vancaester, E, De Blauwe, S, et al. Distinction between contrast staining and hemorrhage after endovascular stroke treatment: one CT is not enough. *J Neurointerv Surg.* (2017) 9:394–8. doi: 10.1136/neurintsurg-2016-012290
- 13. Portela de Oliveira, E, Chakraborty, S, Patel, M, Finitsis, S, and Iancu, D. Value of high-density sign on CT images after mechanical thrombectomy for large vessel occlusion in predicting hemorrhage and unfavorable outcome. *Neuroradiol J.* (2021) 34:120–7. doi: 10.1177/1971400920975259
- 14. Shao, Y, Xu, Y, Li, Y, Wen, X, and He, X. A new classification system for Postinterventional cerebral Hyperdensity: the influence on hemorrhagic transformation and clinical prognosis in acute stroke. *Neural Plast.* (2021) 2021:1–12. doi: 10.1155/2021/6144304
- 15. Lee, MJ, Zhu, J, An, JH, Lee, SE, Kim, TY, Oh, E, et al. A transcriptomic analysis of cerebral microvessels reveals the involvement of Notch1 signaling in endothelial

- mitochondrial-dysfunction-dependent BBB disruption. Fluids Barriers CNS. (2022) 19:64. doi: 10.1186/s12987-022-00363-7
- 16. Wang, Z, Zhou, X, Xu, Y, Fan, S, Tian, N, Zhang, W, et al. Development of a novel dual-order protein-based Nanodelivery carrier that rapidly targets low-grade gliomas with microscopic metastasis in vivo. ACS Omega. (2020) 5:20653–63. doi: 10.1021/acsomega.0c03073
- 17. Erickson, MA, Shulyatnikova, T, Banks, WA, and Hayden, MR. Ultrastructural remodeling of the blood-brain barrier and neurovascular unit by lipopolysaccharide-induced Neuroinflammation. *Int J Mol Sci.* (2023) 24:1640. doi: 10.3390/ijms24021640
- 18. Lee, JM, Lee, JH, Song, MK, and Kim, YJ. NXP031 improves cognitive impairment in a chronic cerebral hypoperfusion-induced vascular dementia rat model through Nrf2 signaling. *Int J Mol Sci.* (2021) 22:6285. doi: 10.3390/ijms22126285
- 19. Wang, DD, Lv, H, and Di, W. Research progress on the mechanism of CT high density imaging after mechanical thrombectomy. *Neurol Dis Mental Health*. (2022) 22:596–60. doi: 10.3969/j.issn.1009-6574.2022.08.012
- 20. Liu, BY, Pan, XH, Zhu, FY, Chen, XM, Liu, ZH, Liu, S, et al. Predicting hemorrhagic transformation value of postinterventional flat-panel CT for patients with acute ischemic stroke after thrombectomy. *Diagn Imaging Interventional Radiol.* (2023) 32:96–102. doi: 10.3969/j.issn.1005-8001.2023.02.003
- 21. Wang, HY, Jian, YT, Zhao, LL, Li, T, Zhang, YH, Dang, MJ, et al. Morphological mechanism of reversibly increased vascular permeability of Ioversol to the blood-brain barrier. *J Stroke Neurol Dis.* (2021) 38:201–4. doi: 10.19845/j.cnki.zfysjjbzz.2021.0051
- 22. Bai, X, Zhang, X, Wang, J, Zhang, Y, Dmytriw, AA, Wang, T, et al. Factors influencing recanalization after mechanical Thrombectomy with first-pass effect for acute ischemic stroke: a systematic review and Meta-analysis. *Front Neurol.* (2021) 12:628523. doi: 10.3389/fneur.2021.628523
- 23. Li, L, Ding, YS, Zuo, P, and Fan, L. Curative effect of mechanical thrombectomy in the treatment of anterior circulation acute large vessel occlusion cerebral infarction and the influencing factors for poor prognosis in patients with vascular recanalization. *Chin J Pract Neurol Dis.* (2023) 26:605–9. doi: 10.12083/SYSJ.221802
- 24. Zhang, Z, Song, C, Zhang, L, and Yang, W. Predictive modeling of short-term poor prognosis of successful reperfusion after endovascular treatment in patients with anterior circulation acute ischemic stroke. *J Healthc Eng.* (2022) 2022:1–9. doi: 10.1155/2022/3185211
- 25. Yang, J, and Gao, Y. Clinical relevance of serum omentin-1 levels as a biomarker of prognosis in patients with acute cerebral infarction. *Brain Behav.* (2020) 10:e01678. doi: 10.1002/brb3.1678
- 26. Powers, WJ, Derdeyn, CP, Biller, J, Coffey, CS, Hoh, BL, Jauch, EC, et al. 2015 American Heart Association/American Stroke Association focused update of the 2013 guidelines for the early management of patients with acute ischemic stroke regarding endovascular treatment. *Stroke.* (2015) 46:3020–35. doi: 10.1161/STR.000000000000000074
- 27. Fu, TY, Ma, CY, Guo, QZ, Sun, DP, Shi, L, Yu, HN, et al. Risk factors analysis of 90-day death in elderly with anterior circulation AIS undergoing endovascular treatment with successful recanalization. *Zhongguo Lao Nian Xin Xue Guan Bing Za Zhi*. (2023) 25:276–80. doi: 10.3969/j.issn.1009-0126.2023.03.013